

## Investigation of void nucleation and propagation during electromigration of flip-chip solder joints using x-ray microscopy

S. H. Chiu and Chih Chen

Citation: [Applied Physics Letters](#) **89**, 262106 (2006); doi: 10.1063/1.2425040

View online: <http://dx.doi.org/10.1063/1.2425040>

View Table of Contents: <http://scitation.aip.org/content/aip/journal/apl/89/26?ver=pdfcov>

Published by the [AIP Publishing](#)

---

### Articles you may be interested in

[Effect of void propagation on bump resistance due to electromigration in flip-chip solder joints using Kelvin structure](#)

Appl. Phys. Lett. **91**, 132113 (2007); 10.1063/1.2790376

[Effect of Al-trace degradation on Joule heating during electromigration in flip-chip solder joints](#)

Appl. Phys. Lett. **90**, 082103 (2007); 10.1063/1.2644061

[Study of void formation due to electromigration in flip-chip solder joints using Kelvin bump probes](#)

Appl. Phys. Lett. **89**, 032103 (2006); 10.1063/1.2226989

[Infrared microscopy of hot spots induced by Joule heating in flip-chip SnAg solder joints under accelerated electromigration](#)

Appl. Phys. Lett. **88**, 022110 (2006); 10.1063/1.2151255

[Effect of current crowding and Joule heating on electromigration-induced failure in flip chip composite solder joints tested at room temperature](#)

J. Appl. Phys. **98**, 013715 (2005); 10.1063/1.1949719

---

The advertisement features a dark blue background with white and orange text. At the top left, it reads 'NEW! Asylum Research MFP-3D Infinity™ AFM' in white, with 'Unmatched Performance, Versatility and Support' in orange below it. On the right, the 'OXFORD INSTRUMENTS' logo is shown in white, with the tagline 'The Business of Science®' underneath. The central part of the ad is divided into four quadrants, each with an image and text: top-left shows a textured surface with the text 'Stunning high performance'; top-right shows a brown, porous-looking surface with 'Simpler than ever to GetStarted™'; bottom-left shows a pattern of circular spots with 'Comprehensive tools for nanomechanics'; bottom-right shows a grid of small, colorful rectangular samples with 'Widest range of accessories for materials science and bioscience'. On the far right, there is a photograph of the MFP-3D Infinity AFM instrument, which is a white and blue boxy device with a microscope-like head on top.

## Investigation of void nucleation and propagation during electromigration of flip-chip solder joints using x-ray microscopy

S. H. Chiu and Chih Chen<sup>a)</sup>

Department of Material Science and Engineering, National Chiao Tung University, Hsin-chu 30050, Taiwan, Republic of China

(Received 21 September 2006; accepted 26 November 2006; published online 27 December 2006)

X-ray microscopy was employed to investigate void nucleation and propagation during electromigration in solder joints. The shape of the voids at various stages can be clearly observed. The voids became irregular when they propagated to deplete the contact opening. Growth velocity at the early stage was found to be  $1.3 \mu\text{m}/\text{h}$  under  $6.5 \times 10^3 \text{ A}/\text{cm}^2$  at  $150^\circ\text{C}$ , and it decreased to  $0.3 \mu\text{m}/\text{h}$  at later stages. Formation of intermetallic compound (IMC) and compositional changes at the interface of solder/IMC on the chip side were attributed to the retarded growth rate at later stages. © 2006 American Institute of Physics. [DOI: 10.1063/1.2425040]

To meet the demand for higher performance in portable microelectronic device applications, flip-chip technology has been adopted for high-density packaging due to its excellent electrical characteristics and superior heat dissipation capability. With the increase in the required performance in microelectronic devices, the current that each bump has to carry is also on the increase.<sup>1</sup> The corresponding current density may reach  $1 \times 10^4 \text{ A}/\text{cm}^2$  in the near future. Under such a high current density at the solder bump, electromigration inevitably becomes a critical reliability issue.<sup>2,3</sup>

During electromigration, voids nucleate in the solder bump near the point of entry of electron flow, where serious current crowding and flux divergence occur.<sup>4-7</sup> With the increase in stressing time, void propagates towards the rest of the under bump metallization (UBM) opening, resulting in open failure of the joints. In previous studies, void formation and propagation were observed by cross-sectional scanning electron microscope (SEM). Therefore, only the length and the depth of the void at those specific cross sections can be observed. However, the location where voids nucleate, the shape of voids, as well as how voids propagate in the UBM opening remain unclear. In addition, the propagation velocities of voids at different stages have not been measured.

X-ray microscopy has been employed to study formation of voids in Cu interconnects during electromigration.<sup>8</sup> Since the size of voids formed in Cu interconnects is in submicron range, synchrotron radiation x ray is needed. For flip-chip solder joints, the voids are of a much larger dimension, typically ranging from few microns to tens of microns. Thus, a laboratory-based x-ray microscope appears to be sufficient for the investigation of void nucleation and propagation in solder joints during electromigration. Nevertheless, it has not been applied to solder joints.

In this letter, void formation during electromigration was monitored by an x-ray microscope. The area of the voids was measured from the x-ray images, with which the velocity of void propagation was calculated. This approach provides a deeper understanding on the behavior of void nucleation and propagation during electromigration in solder joints.

Figure 1(a) shows the cross-sectional schematic for the solder joint used in this study. The Al trace was  $1.5 \mu\text{m}$  thick and  $100 \mu\text{m}$  wide, while Cu lines on the substrate were  $25 \mu\text{m}$  thick and  $100 \mu\text{m}$  wide. The UBM consists of  $0.1 \mu\text{m}$  Ti,  $5 \mu\text{m}$  Cu, and  $3 \mu\text{m}$  Ni layers. The diameters of the UBM and the passivation openings were  $120$  and  $85 \mu\text{m}$ , respectively. Electroplated SnPb solder bumps were mounted on an FR4 substrate to form flip-chip joints. Non-solder-mask-defined process was used in this structure. The dimension of the Cu pad opening was  $300 \mu\text{m}$  in diameter. Owing to the large opening in the substrate side, the bump height was as small as  $25 \mu\text{m}$ . With the low bump height, the voids in the solder bump would be much clearly seen in an x-ray microscope. The solder joints were stressed by  $0.8 \text{ A}$  at  $150^\circ\text{C}$  for a desired time. The direction of the electron flow was indicated by the arrows in the figure. Then they were examined by a Dage XL-6500 x-ray microscope with the Si side facing the x-ray detector, whose spatial resolution is  $2 \mu\text{m}$ . The corresponding current density was  $6.5 \times 10^3 \text{ A}/\text{cm}^2$ . The operation voltage was set at  $95 \text{ kV}$  in this study. Since voids form in the bump with electron flow from the chip side to the substrate side, only the bumps with this stressing direction were examined. SEM was also employed to examine the voids in the cross section of the solder bumps.

The shape of the voids induced by electromigration can be clearly observed using x-ray microscope. Figure 2(a) shows the x-ray image of the solder joints before current

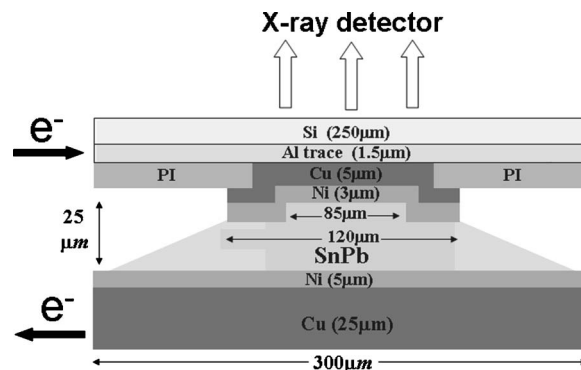


FIG. 1. Cross-sectional schematic diagram of the samples used in this study.

<sup>a)</sup> Author to whom correspondence should be addressed; electronic mail: chih@faculty.nctu.edu.tw

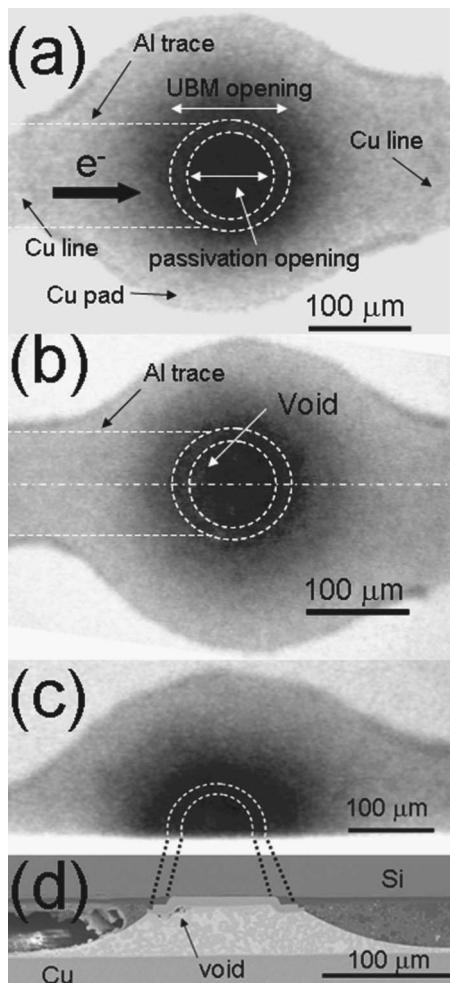


FIG. 2. (a) Plan-view x-ray image of the joint before current stressing. The UBM and passivation openings were labeled by the dotted white circles. (b) X-ray image of the same joint after current stressing. The void was enclosed by the white line. (c) X-ray image of the same joint after being polished laterally to middle of the joint. (d) Cross-sectional SEM image of the joint in (c). A void formed near the entrance of the Al trace.

stressing. Since the Al trace is quite thin and the density of Al is low, it is not visible in the x-ray image. The position of the Al trace was denoted by the two dashed lines in Fig. 2(a). Since the Cu line in the substrate was as thick as 25 μm, it was visible in the x-ray image. To facilitate the observation of void formation, the passivation and UBM openings were marked on the image by two dotted white circles. The center region shows a darker image due to the Cu/Ni UBM and thicker solder in this region. After current stressing at 0.8 A at 150 °C for 29.8 h, the same sample was examined again by x-ray microscope. A small brighter region was observed near the left corner of the UBM opening, where the electrons crowded into the solder bump. Furthermore, the voids extended backwards to the UBM opening because the UBM layer may serve as a conducting path for electrons.<sup>6,9</sup> The shape of void appears to be irregular. This specimen was labeled as sample A in this letter. To verify if voids were formed in this region, the sample was ground and polished laterally to approximate the center of the bump, and it was inspected again by x-ray microscope, as shown in Fig. 2(c). The location of the cross section is also indicated by the middle dashed line in Fig. 2(b). Then it was examined by SEM to reveal the location of voids, as shown in Fig. 2(d). As can be seen, the void position matched that obtained by

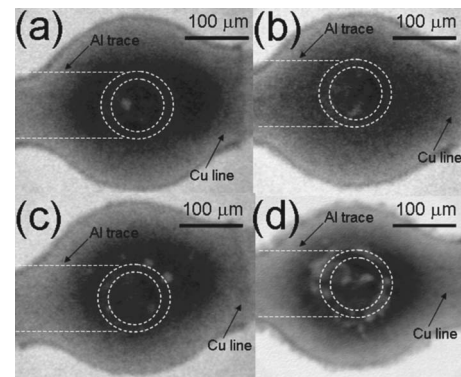


FIG. 3. Plan-view x-ray images of the joint after stressing for (a) 37.8 h, (b) 110.2 h, (c) 177.8 h, and (d) 384.0 h. The position of the Al trace was labeled by the dotted lines in the figures.

x-ray microscope. Therefore, x-ray microscopy can be employed to observe void formation.

The growth velocity of the voids can be calculated from the x-ray images. To obtain the growth velocity at different stages, four more samples were stressed for different lengths of time and then examined by x-ray microscopy and SEM. They were labeled as samples B–E in this letter. Figures 3(a)–3(d) show the x-ray images of the four samples stressed at 0.8 A at 150 °C for 37.8, 110.2, 177.8, and 384.0 h, respectively. The corresponding SEM images were shown in Figs. 4(a)–4(d). Larger voids were formed with the increase in stressing time, and the voids propagated from the left-hand side to the right-hand side. In addition, the voids became irregular as they propagated, as shown in Figs. 3(b)–3(d). The heights of the voids were larger. Thus, the void contrast was better for the x-ray image. SEM image shows that thicker intermetallic compounds (IMCs) of Ni<sub>3</sub>Sn<sub>4</sub> were formed between the Ni UBM and solder, as indicated by the arrows in the SEM images in Figs. 4(c) and 4(d). Both x-ray and SEM images indicate that the voids in samples D and E became discontinuous. Because the IMC has better electromigration resistance than the solder, void propagation would be hindered by the IMC grains. To calculate the growth velocity of the voids, the area of voids was calculated from the x-ray images by a computer software. Figure 5(a) shows the area of voids as a function of stressing

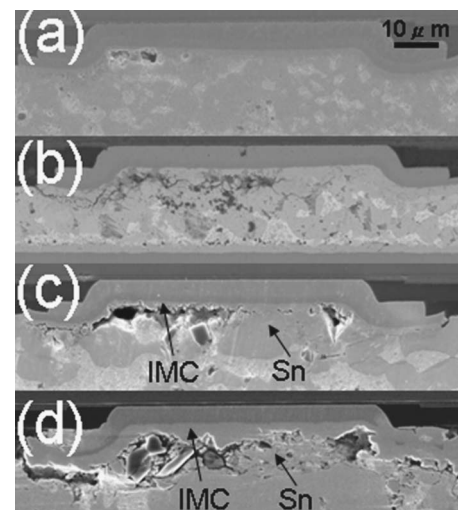


FIG. 4. Corresponding cross-sectional SEM images of the joint in Figs. 3(a)–3(d).

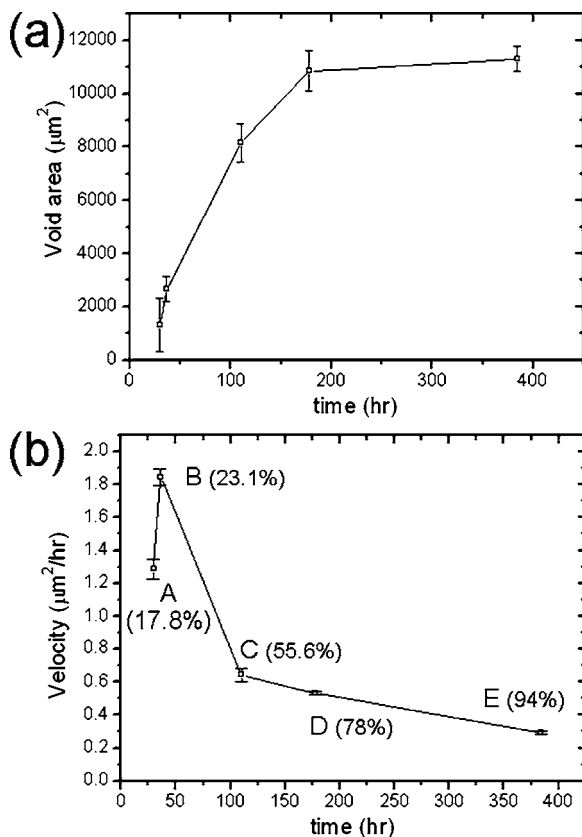


FIG. 5. (a) Plot of depletion area as a function of stressing time. (b) Plot of void growth velocity against stressing time for the five samples. The depletion percentage of UBM opening for each sample was also shown in the figure.

time for the above five samples, and it increased with the increase in stressing time. The slope between the first two points was higher. The reason will be discussed later. To calculate the average growth velocity, the maximum length along the propagation direction, which is the positive  $X$  axis, was adopted as the propagation length. Then the growth velocity was calculated on the basis of the void propagation length and the stressing time. Figure 5(b) illustrates the average growth velocity for the five samples. It is found that the average growth velocity was  $1.3 \mu\text{m}/\text{h}$  for sample A. It increased to  $1.8 \mu\text{m}/\text{h}$  for sample B, and it decreased to  $0.6 \mu\text{m}/\text{h}$  for sample C,  $0.5 \mu\text{m}/\text{h}$  for sample D, and  $0.3 \mu\text{m}/\text{h}$  for sample E. In addition, the depletion percentages of UBM opening were 17.8%, 23.1%, 55.6%, 78.0%, and 94.0% for the five samples, as labeled in Fig. 5(b).

The incubation time for void formation may be responsible for the low growth velocity for sample A in the initial stage. Under the condition of current stressing, the incubation time was about 20 h for the solder joints used in this study. Only a small void was formed in sample A. Therefore, the velocity was low for sample A. Once the voids were formed, they propagated more quickly, as shown in sample B. The measured velocity was 1.4 times faster than that of sample A. However, the velocity decreased for samples C, D–E. The above findings are quite different from those for Al and Cu interconnects. At later stages of electromigration in Al and Cu interconnects, the growth rate of voids became higher due to the much higher current density around the

voids. In addition, for solder joints with thin-film UBM, the voids also grew faster at later stages.<sup>10</sup> It is speculated that IMC formation and compositional changes may be responsible for the low velocities of our samples at later stages. For the former,  $\text{Ni}_3\text{Sn}_4$  may inhibit void propagation, as shown in Figs. 4(c) and 4(d). For the latter, solder composition at the IMC/solder interface changes to pure Sn at later stages, as also shown in Figs. 4(c) and 4(d). Since pure Sn has higher electromigration resistance than eutectic solder,<sup>11</sup> void propagation would be slowed down at later stages. In addition, it is reported that the current crowding effect is relieved as the voids propagate before depleting half of the UBM opening,<sup>9</sup> since the current is spread out more uniformly in the Al pad directly above the voids. For sample E, current crowding effect became worse, yet the growth rate decreased to  $0.3 \mu\text{m}/\text{h}$ , indicating that IMC formation and compositional change dominated the growth velocity of voids.

Compared with the growth velocity reported by Zhang *et al.*, the value obtained in this study was slightly smaller. Their testing conditions were  $3.67 \times 10^3 \text{ A}/\text{cm}^2$  at  $146^\circ\text{C}$  on 95.5Sn–4.0Ag–0.5Cu solder joints with Al/Ni(V)/Cu thin-film UBM. The growth velocity of voids they obtained was about  $4.4 \mu\text{m}/\text{h}$ . In contrast, our testing conditions were  $6.5 \times 10^3 \text{ A}/\text{cm}^2$  at  $150^\circ\text{C}$ , which are more severe than theirs. It is speculated that the thick UBM layer may slow down void propagation. The UBM used in this study was  $5 \mu\text{m Cu}/3 \mu\text{m Ni}$ . It is reported that this thick UBM layer can relieve the current crowding effect by a factor of 3.3 times, compared with Al/Ni(V)/Cu thin-film UBM. Therefore, the growth velocity of voids was slower for solder joints with a thick-film UBM.

In summary, x-ray microscopy can detect void nucleation and propagation in flip-chip solder joints. The voids nucleated in the vicinity of the entrance point of Al trace, and their shape was quite irregular. The growth velocity was measured to be around  $0.3\text{--}1.8 \mu\text{m}/\text{h}$  at various stages under  $6.5 \times 10^3 \text{ A}/\text{cm}^2$  at  $150^\circ\text{C}$  for SnPb solder joints with thick-film Cu/Ni UBM.

The authors would like to thank National Science Council of Taiwan of R.O.C. for the financial support through Grant No. NSC 95-2218-E-009-022.

<sup>1</sup>K. N. Tu, *J. Appl. Phys.* **94**, 5451 (2003).

<sup>2</sup>International Technology Roadmap for Semiconductors, Assembly and Packaging Section, Semiconductor Industry Association, San Jose, CA, 2003, pp. 4–9.

<sup>3</sup>C. Y. Liu, Chih Chen, C. N. Liao, and K. N. Tu, *Appl. Phys. Lett.* **75**, 58 (1999).

<sup>4</sup>Everett C. C. Yeh, W. J. Choi, and K. N. Tu, *Appl. Phys. Lett.* **80**, 4 (2002).

<sup>5</sup>J. W. Nah, K. W. Paik, J. O. Suh, and K. N. Tu, *J. Appl. Phys.* **94**, 7560 (2003).

<sup>6</sup>L. Zhang, S. Ou, J. Huang, K. N. Tu, St. Gee, and L. Nguyen, *Appl. Phys. Lett.* **88**, 012106 (2006).

<sup>7</sup>Y. W. Chang, S. W. Liang, and Chih Chen, *Appl. Phys. Lett.* **89**, 032103 (2006).

<sup>8</sup>G. Schneider, G. Denbeaux, E. H. Anderson, B. Bates, A. Pearson, M. A. Meyer, E. Zschech, D. Hambach, and E. A. Stach, *Appl. Phys. Lett.* **81**, 2535 (2002).

<sup>9</sup>S. W. Liang, Y. W. Chang, T. L. Shao, Chih Chen, and K. N. Tu, *Appl. Phys. Lett.* **89**, 022117 (2006).

<sup>10</sup>W. J. Choi, E. C. C. Yeh, and K. N. Tu, *J. Appl. Phys.* **94**, 5665 (2003).

<sup>11</sup>C. Y. Liu, Chih Chen, and K. N. Tu, *J. Appl. Phys.* **88**, 5703 (2000).